No evidence of phosphine in the atmosphere of Venus by independent analyses

Villanueva G.L., Cordiner, M., Irwin P., de Pater I., Butler B., Gurwell M., Milam S.N., Nixon C. A., Luszcz-Cook S. H., Wilson C.F., Kofman V., Liuzzi G., Faggi S., Fauchez T., Lippi M., Cosentino R., Thelen A. E., Moullet A., Hartogh P., Molter E.M., Charnley S., Arney G.N., Mandell A.M, Biver N., Vandaele A.C., de Kleer K. R., Kopparapu R.

The detection of phosphine (PH_3) in the atmosphere of Venus has been recently reported based on millimeter-wave radio observations[1] (G2020a hereafter), and its re-analyses[2,3] (G2021a/b thereafter). In this note we perform an independent re-analysis, identifying several issues in the interpretation of the spectroscopic data. As a result, we determined sensitive upper-limits for PH_3 in Venus' atmosphere (>75 km, above the cloud decks) that are discrepant with the findings in G2020 and G2021a/b [please change it throughout the paper].

The measurements target the fundamental first rotational transition of PH_3 (J=1-0) at 266.944513 GHz, which was observed with the James Clerk Maxwell Telescope (JCMT) in June 2017 and with the Atacama Large Millimeter/submillimeter Array (ALMA) in March 2019. This line's center is near the SO_2 ($J=30_{9,21}-31_{8,24}$) transition at 266.943329 GHz (only 1.3 km/s away from the PH_3 line) which represents a potential source of contamination. The JCMT and ALMA data, as presented in G2020a/b, are at spectral resolutions comparable to the frequency separation of the two lines. Moreover, the spectral features identified are several km/s in width, and therefore do not permit distinct spectroscopic separation of the candidate spectral lines of PH_3 and SO_2. We present the radiative transfer modelling we have performed and then discuss the ALMA and JCMT analyses in turn.

ALMA reanalysis: The analysis of interferometric data is relatively complex, in particular for bright and extended sources such as Venus (15.2 arcsecs angular diameter for the ALMA data). The completeness of the different baselines (short and long) determines the ability to accurately measure the total planetary flux density[9], while the bandpass calibration is a crucial factor in the ultimate quality of the resulting spectra[10,11]. The details of the calibration and imaging used during data reduction can have a dramatic impact on the quality and validity of the resulting ALMA interferometric data. The extracted spectra in "extended Figure 4" and interferometric map in "extended Figure 3" of G2020a show large quasi-periodic fluctuations in the spectrum, which in G2020a/b is fitted with high-order polynomials. Particularly challenging is the fact that these fluctuations have a pattern/width comparable to their defined PH_3 line core region. As we present in S2 and also reported in [12,13], artificially produced features which mimic true atmospheric lines can be produced when removing high-order polynomials from data with such characteristics.

Many of these large fluctuations can be introduced by the particular parameters used in calibration during data reduction. For instance, after the initial release of the data and data reduction scripts, we independently reduced the data in several different ways, and observed substantial differences in the final spectra when applying different treatments of the bandpass calibrations. Specifically, the type of bandpass calibration solution (traditional channel-to-channel vs. polynomial-fitted vs. smoothed), and in particular, enabling the "usescratch=True"

setting in CASA's `setJy` for the model used for Callisto (the bandpass calibrator). After our initial independent analyses of the data in September-October 2020, we notified the ALMA NAASC team of these issues. Ultimately, the Joint ALMA Office (JAO) decided to independently re-process the data and released updated scripts and data products in November 2020, upon which the G2020b analysis is based. Beyond our original analysis of the data in which we could not recover a PH_3 signature (see Figure 1B), we have also independently reduced the ALMA data using these new JAO scripts as the starting point. We employed three separate procedures by three different groups (NASA/GSFC, Berkeley, and NRAO), making use of different methods in order to evaluate the significance of the reported ALMA PH_3 signatures. The three methods are: 1) employing the updated JAO scripts throughout (using CASA only, done at NASA/GSFC); 2) employing the updated JAO scripts, but proceeding independently beyond self-calibration (using CASA only; done at Berkeley) – note that phase-only self-calibration was done but not amplitude self-calibration, because the latter can be problematic for extended sources[9]; 3) as (2), but with the post-JAO-script reduction done in AIPS (using both CASA and AIPS, done at NRAO). We investigated including/removing certain baselines, with further details about the methods can be found in S2. All these analyses used the common foundation of the revised JAO scripts to do the initial calibration (in particular, the bandpass and complex gain vs. time calibrations), and very similar steps in the further data reduction (phase-only self-calibration, continuum subtraction, forming the image cube, and extracting the disk-averaged spectrum).

The quality of the bandpass calibration was improved with the updated JAO scripts, yet the residual spectrum still showed notable large fluctuations (we found that a 6^{th} order polynomial captured most of the residual large fluctuations for method 1; G2020b considered a 12^{th} order). Our other two re-analyses (2 and 3) led to practically flat spectra only needing 2^{nd} order polynomial baselines (more information on the origin of these differences is explained in S2). Ultimately, all our analyses of the data using these different approaches and methodologies reveal no conclusive signature of PH_3 (Figure 1), leading to an upper-limit of < 1 ppbv (3σ) when employing a linewidth of 0.186 cm^{-1}/atm. When employing other proposed linewidths, the upper-limit would be PH_3 < 0.7 ppbv (linewidth of 0.12 cm^{-1}/atm) or < 1.5 ppbv (linewidth of 0.286 cm^{-1}/atm). This upper-limit is also consistent with other recently reported upper-limits derived from IR ground-based observations (PH_3 < 5 ppbv)[14] and from spacecraft data (PH_3 < 0.2 ppbv)[15]. We further validated our analysis of the ALMA data by analyzing other SO_2 and HDO lines in the same dataset (see S3).

JMCT analysis and SO2 contamination: The analysis of JCMT spectral data in G2020a involved fitting of multiple polynomials for the purpose of continuum subtraction: an initial 4^{th} order polynomial was removed, then a 9^{th} order polynomial was removed from a smoothed spectrum, and finally a masked 8^{th} order polynomial was removed. Recently, Thompson[13] explored the robustness of the two detection methods used in G2020a, namely low order polynomial fits and higher order multiple polynomial fits, and found that neither line detection method is able to recover a statistically significant detection at the position of the PH_3/SO_2 line.

We investigate whether a weak PH_3 signature, if present, could be distinguished from SO_2 contamination, and what its contribution to the detected signal could be. To explore this, we employed the same VIRA45 temperature/pressure (T/P) profile used by G2020a ("extended Data

Figure 8") and the G2020a SO_2 profile presented in "extended Data Figure 9" (~100 ppbv in the 70-90 km region, dropping to <30 ppbv above 95 km). If this potential SO_2 contaminant signature is removed from the JCMT data, then the original feature would be confined within the noise (Fig. 2). We next modelled a mesospheric SO_2 profile as measured by Venus Express using solar occultation[16], and similar to case D of ref [17] (SO_2 abundance of ~30 ppbv at 80 km, increasing to ~100 ppb at 90 km and reaching ~300 ppbv at 95 km). In this case, the SO_2 contamination signature is even stronger and fully captures the claimed PH_3 residual in G2020a/b/c (Fig. 2). A comprehensive compilation of SO_2 measurements[12-13], including thousands of measurements from the Venus Express orbiter in UV and IR wavelengths as well as ground-based observations[16,18–27], show that SO_2 abundances at 80 km are frequently well in excess of 100 ppbv, with peak abundances occasionally exceeding 1000 ppbv. This shows that the SO_2 profiles we adopted are well within usual ranges of variability observed on Venus (more information about the considered profiles can be found in S1). Having shown that the absorption line can be reproduced by reasonable vertical profile of SO_2, we therefore argue that this absorption line cannot be definitively attributed to PH_3.

Probing altitude: We also explored the altitudes from which these absorptions originate, which can be used to constrain photochemical models and facilitate comparison to other measurements[28,29]. This is ultimately related to the spectroscopic parameters of the targeted line and that of the competing radiative active species in this spectral region. When considering the linewidth of 0.186 cm^{-1}/atm for PH_3, at 70 km ($3.4x10^{-2}$ atm) the line would be 213 km/s wide, i.e., much broader than the narrow window region of ±5 km/s or ±10 km/s searched for PH_3. As a polynomial is fitted and subtracted, removing any spectral line information beyond this core region, the spectral information at broader widths (originating from lower altitudes) is thus removed. Our models only predict an observable PH_3 absorption at this frequency only when phosphine is present above 75 km (see details in S4), and therefore these data provide no constraints on its abundance in the cloud deck (50-70 km), in contrast to G2020a/b. This can be seen in Fig. 2, a flat spectrum is calculated for the PH_3 profile determined from the chemical modelling described in G2020a, in which PH_3 is present only below 70 km altitude.

Conclusions: By our independent analysis of the ALMA data, we set an limit of 1 ppbv for PH_3.. We also show that the observed JCMT feature could be attributed to mesospheric SO_2 gas. Furthermore, for any PH_3 signature to be recoverable in either ALMA or JCMT analyses, PH_3 needs to be present at altitudes above 75 km. We conclude that the recent identification of PH_3 in the upper atmosphere of Venus is not supported

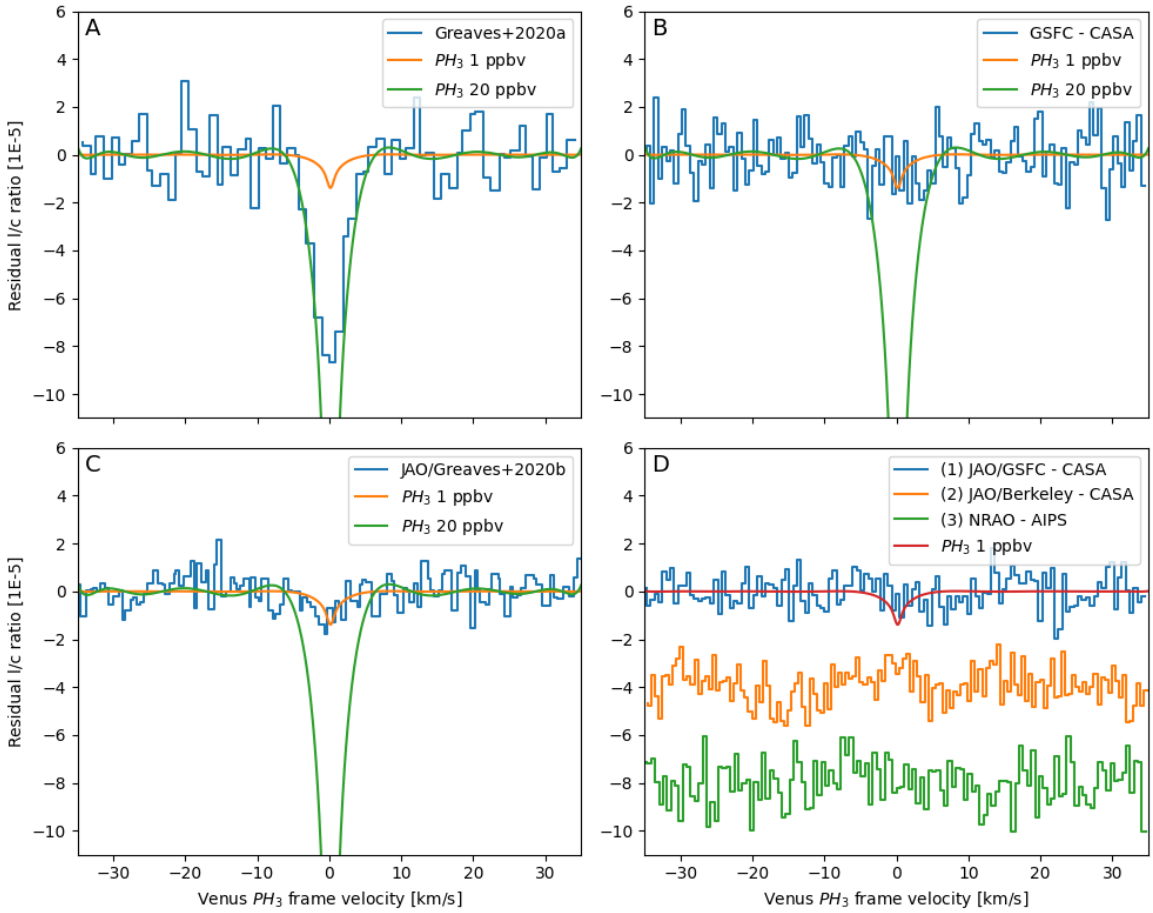

Figure 1: Comparison between the ALMA data as presented in G2020a/b and our independent analyses of the same data retrieved from the ALMA science archive. Models with constant 1 and 20 ppbv PH_3 abundances are superposed. **Panel A**: The ALMA data as presented in Figure 2 of G2020a for the whole planet (dv:1 km/s). **Panel B:** Our original analysis of the raw ALMA data (dv:0.55 km/s), employing the original G2020a scripts but enabling the "usescratch=True" setting in CASA's `setJy`, correcting the bandpass calibration. **Panel C**: The re-analyzed data presented in G2020b using updated scripts, yet G2020b employed a higher (12^{th} order) polynomial in the bandpass calibration (instead of 3^{rd} order in the JAO script), and excluded short baselines (<33 m) from their analysis (dv: 0.55 km/s). **Panel D**: Our independent analysis of the JAO-revised ALMA data, employing different methods, a resolution of dv:0.55 km/s, methods 1 and 2 including all baselines and method 3 excluding <33 m baselines. A 6^{th} order polynomial was removed for (1), see details in S2, while only a 2^{nd} was removed for (2) and (3).

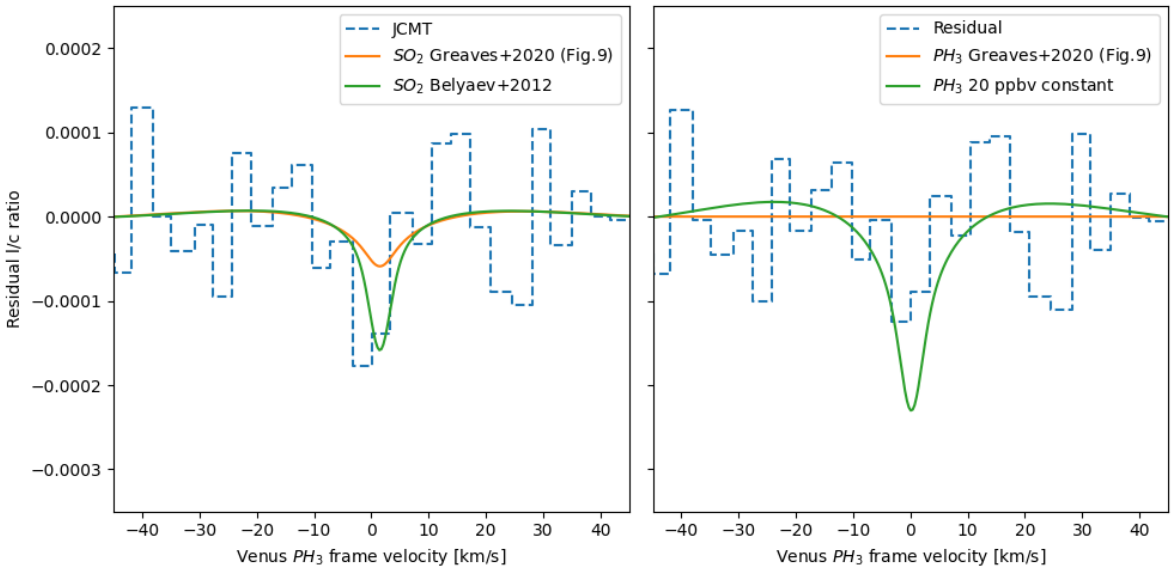

Figure 2: Comparison between the residual JCMT data as presented in Figure 1 of G2020a and models of SO_2 and PH_3. **Left**: The JCMT data for their mid-range solution with masking within ± 5 km/s, while "SO_2 Greaves+2020" is a model spectrum synthesized using the T/P in G2020a/Fig. 8 and the SO_2 profile in G2020a/Fig. 9. "SO_2 Belyaev+2012" is a typical profile in Belyaev+2012[16] (Fig. 9) and similar to Lincowski+2021[17] (case D), with an SO_2 abundance of ~30 ppbv at 80 km, and increasing to ~100 ppbv at 90 km and reaching ~300 ppb at 95 km. **Right**: "Residual" is obtained by removing the SO_2 signature from the JCMT data as modelled with a 3 km/s resolution using the G2020a/Fig. 9 SO_2 profile. The "PH_3 Greaves+2020" spectrum is a model spectrum employing the PH_3 profile in G2020a/Fig. 9 (peaking at 60 km with 20 ppbv) and the default linewidth (0.186 cm^{-1}/atm), while a model considering a vertically constant mixing ratio of 20 ppbv is labelled "PH_3 20 ppbv constant". The "PH_3 Greaves+2020" is flat and featureless because these measurements only sample PH_3 above 75 km (see S4).

Methods

We have employed three independent radiative transfer models: the Planetary Spectrum Generator (PSG, https://psg.gsfc.nasa.gov)[4], the Non-linear optimal Estimator for MultivariatE spectral analySIS (NEMESIS)[5] and the CfA planetary modeling tool[6]. The PSG radiative transfer analysis included the latest HITRAN SO_2 line parameters for a CO_2 atmosphere[7], a layer-by-layer, line-by-line study, and a full disk sampling scheme with 10 concentric rings. The NEMESIS analysis was also performed in line-by-line mode, and used the same spectroscopic data with a 5-point Gauss-Lobatto disc-integration scheme. As described in G2020a/b, there is some uncertainty in the line-shape parameters for the PH_3 line in a CO_2 atmosphere. HITRAN reports an air linewidth of 0.067 cm^{-1}/atm, which would correspond to 0.12 cm^{-1}/atm in a CO_2 atmosphere if the value is scaled by the typical 1.8 scaling ratio observed for the SO_2 lines[8]. G2020a considered a theoretical estimate of 0.186 cm^{-1}/atm, and an upper range of 0.286 cm^{-1}/atm measured for the NH_3(J=1-0) line in CO_2 at 572.498160 GHz. Considering the uncertainty on this parameter, we adopt the same value in G2020a by default (0.186 cm^{-1}/atm).

[as a side note, you could consider moving the text currently in the Supplementary Material to the Methods, so that it is part of the paper and not in an aside file. But that's not mandatory. Something I would ask, though, is to rename the supplementary figures as "Supplementary Figure 1" and not "Figure FS1" –and cite them as such]

Acknowledgements and data availability

This paper makes use of the 2018.A.00023.S ALMA data, available at https://almascience.nrao.edu/asax. We would like to commend the G2020a team for making their data and scripts available. ALMA is a partnership of ESO (representing its member states), NSF (USA) and NINS (Japan), together with NRC (Canada), MOST and ASIAA (Taiwan), and KASI (Republic of Korea), in cooperation with the Republic of Chile. The Joint ALMA Observatory is operated by ESO, AUI/NRAO and NAOJ. The JCMT data was collected under project S16BP007, and available at https://www.eaobservatory.org/jcmt/science/archive. The JCMT is operated by the EAO on behalf of NAOJ; ASIAA; KASI; CAMS as well as the National Key R&D Program of China (No. 2017YFA0402700). Additional funding support is provided by the STFC and participating universities in the UK and Canada. The authors wish to recognize and acknowledge the very significant cultural role and reverence that the summit of Maunakea has always had within the indigenous Hawaiian community. We are most fortunate to have the opportunity to conduct observations from this mountain.

References

1. Greaves, J. S. *et al.* Phosphine gas in the cloud decks of Venus. *Nat. Astron.* 1–10 (2020) doi:10.1038/s41550-020-1174-4.
2. Greaves, J. S. *et al.* Re-analysis of Phosphine in Venus' Clouds. *ArXiv201108176 Astro-Ph* (2020).
3. Greaves, J. S. *et al.* On the Robustness of Phosphine Signatures in Venus' Clouds. *ArXiv201205844 Astro-Ph* (2020).
4. Villanueva, G. L., Smith, M. D., Protopapa, S., Faggi, S. & Mandell, A. M. Planetary Spectrum Generator: An accurate online radiative transfer suite for atmospheres, comets, small bodies and exoplanets. *J. Quant. Spectrosc. Radiat. Transf.* **217**, 86–104 (2018).
5. Irwin, P. G. J. *et al.* The NEMESIS planetary atmosphere radiative transfer and retrieval tool. *J. Quant. Spectrosc. Radiat. Transf.* **109**, 1136–1150 (2008).
6. Gurwell, M. A., Bergin, E. A., Melnick, G. J. & Tolls, V. Mars surface and atmospheric temperature during the 2001 global dust storm. *Icarus* **175**, 23–31 (2005).
7. Gordon, I. E. *et al.* The HITRAN2016 molecular spectroscopic database. *J. Quant. Spectrosc. Radiat. Transf.* **203**, 3–69 (2017).
8. Wilzewski, J. S., Gordon, I. E., Kochanov, R. V., Hill, C. & Rothman, L. S. H2, He, and CO2 line-broadening coefficients, pressure shifts and temperature-dependence exponents for the HITRAN database. Part 1: SO2, NH3, HF, HCl, OCS and C2H2. *J. Quant. Spectrosc. Radiat. Transf.* **168**, 193–206 (2016).
9. Pater, I. de *et al.* First ALMA Millimeter-wavelength Maps of Jupiter, with a Multiwavelength Study of Convection. *Astron. J.* **158**, 139 (2019).
10. Thelen, A. E. *et al.* Detection of CH$_3$C$_3$N in Titan's Atmosphere. (2020).

11. Yamaki, H., Kameno, S., Beppu, H., Mizuno, I. & Imai, H. Optimization by Smoothed Bandpass Calibration in Radio Spectroscopy. *Publ. Astron. Soc. Jpn.* **64**, (2012).
12. Snellen, I. A. G., Guzman-Ramirez, L., Hogerheijde, M. R., Hygate, A. P. S. & van der Tak, F. F. S. Re-analysis of the 267-GHz ALMA observations of Venus: No statistically significant detection of phosphine. *ArXiv201009761 Astro-Ph* (2020).
13. Thompson, M. A. The statistical reliability of 267-GHz JCMT observations of Venus: no significant evidence for phosphine absorption. *Mon. Not. R. Astron. Soc. Lett.* **501**, L18–L22 (2020).
14. Encrenaz, T. *et al.* A stringent upper limit of the PH3 abundance at the cloud top of Venus. *Astron. Astrophys.* **643**, L5 (2020).
15. Trompet, L. *et al.* Phosphine in Venus' atmosphere: Detection attempts and upper limits above the cloud top assessed from the SOIR/VEx spectra. *Astron. Astrophys.* **645**, L4 (2021).
16. Belyaev, D. A. *et al.* Vertical profiling of SO2 and SO above Venus' clouds by SPICAV/SOIR solar occultations. *Icarus* **217**, 740–751 (2012).
17. Lincowski, A. P. *et al.* Claimed detection of PH$_3$ in the clouds of Venus is consistent with mesospheric SO$_2$. *ArXiv210109837 Astro-Ph* (2021).
18. Krasnopolsky, V. A. Spatially-resolved high-resolution spectroscopy of Venus 2. Variations of HDO, OCS, and SO2 at the cloud tops. *Icarus* **209**, 314–322 (2010).
19. Sandor, B. J., Todd Clancy, R., Moriarty-Schieven, G. & Mills, F. P. Sulfur chemistry in the Venus mesosphere from SO2 and SO microwave spectra. *Icarus* **208**, 49–60 (2010).
20. Piccialli, A. *et al.* Mapping the thermal structure and minor species of Venus mesosphere with ALMA submillimeter observations. *Astron. Astrophys.* **606**, A53 (2017).
21. Vandaele, A. C. *et al.* Sulfur dioxide in the Venus atmosphere: I. Vertical distribution and variability. *Icarus* **295**, 16–33 (2017).
22. Vandaele, A. C. *et al.* Sulfur dioxide in the Venus Atmosphere: II. Spatial and temporal variability. *Icarus* **295**, 1–15 (2017).
23. Vandaele, A. C. Composition and Chemistry of the Neutral Atmosphere of Venus. *Oxford Research Encyclopedia of Planetary Science* https://oxfordre.com/planetaryscience/view/10.1093/acrefore/9780190647926.001.0001/acrefore-9780190647926-e-4 (2020) doi:10.1093/acrefore/9780190647926.013.4.
24. Encrenaz, T., Moreno, R., Moullet, A., Lellouch, E. & Fouchet, T. Submillimeter mapping of mesospheric minor species on Venus with ALMA. *Planet. Space Sci.* **113–114**, 275–291 (2015).
25. Encrenaz, T. *et al.* HDO and SO2 thermal mapping on Venus - IV. Statistical analysis of the SO2 plumes. *Astron. Astrophys.* **623**, A70 (2019).
26. Marcq, E. *et al.* Climatology of SO2 and UV absorber at Venus' cloud top from SPICAV-UV nadir dataset. *Icarus* **335**, 113368 (2020).
27. Encrenaz, T. *et al.* HDO and SO2 thermal mapping on Venus - V. Evidence for a long-term anti-correlation. *Astron. Astrophys.* **639**, A69 (2020).
28. Mogul, R., Limaye, S. S. & Way, M. Venus' Mass Spectra Show Signs of Disequilibria in the Middle Clouds. *Earth and Space Science Open Archive* http://www.essoar.org/doi/10.1002/essoar.10504552.1 (2020) doi:10.1002/essoar.10504552.1.
29. Mogul, R., Limaye, S. S., Way, M. J. & Cordova, J. Is Phosphine in the Mass Spectra from Venus' Clouds? *ArXiv200912758 Astro-Ph* (2020).

30. Seiff, A. *et al.* Models of the structure of the atmosphere of Venus from the surface to 100 kilometers altitude. *Adv. Space Res.* **5**, 3–58 (1985).
31. Limaye, S. S. *et al.* Venus Atmospheric Thermal Structure and Radiative Balance. *Space Sci. Rev.* **214**, 102 (2018).
32. Akins, A. B., Lincowski, A. P., Meadows, V. S. & Steffes, P. G. Complications in the ALMA Detection of Phosphine at Venus. *Astrophys. J.* **907**, L27 (2021).